Growth Rate Dispersion in Batch Crystallization

A method for describing the crystal size distribution of a batch crystallizer in the presence of growth rate dispersion is presented. The analysis is based on the assumption that individual crystals have inherent constant growth rates, but the growth rate may vary from crystal to crystal, resulting in a distribution of growth rates. The method requires the availability of growth rate, growth rate dispersion, and nucleation rate expressions for prediction of the crystal size distribution. These required rate expressions can be recovered by the use of simple linear regressions from the CSD moment data. Prediction of the unsteady-state CSD was demonstrated using rate expressions for the sucrose-water system. Batch fructose experiments were analyzed to demonstrate the recovery of the growth and nucleation rates from the size distribution data.

Lie-Ding Shiau
Kris A. Berglund
Department of Chemical Engineering
Department of Agricultural Engineering
Michigan State University
East Lansing, MI 48824

Introduction

The phenomenon of growth rate dispersion (GRD) is a significant factor in the establishment of the crystal size distribution (CSD) in crystallizers. Two methods of modeling GRD have been presented in the literature. The first, in which it is assumed that the growth rate of an individual crystal fluctuates in the course of time, is referred to as the random fluctuation (RF) model (Randolph and White, 1977). In the second, based on the contact nucleation studies of Berglund and Larson (1981), Ramanarayanan (1982), and Berglund et al. (1983), it is assumed that individual crystals have inherent, constant growth rates, but different crystals have different inherent growth rates. This model will be referred to as the constant crystal growth (CCG) model.

Results supporting the RF model have been observed in a few studies over long time periods up to 15 days (Garside, 1985). However, the CCG model has been found to be applicable in a number of systems for periods of a few hours (Garside, 1985; Berglund, 1986; Shiau and Berglund, 1987; Chu et al., 1989) through the photomicroscopic technique developed by Garside and Larson (1978). Berglund (1986) concluded that GRD is a widespread phenomenon in contact nuclei of soluble materials, and the CCG model applies in both inorganic and organic aqueous systems as well as those systems with large and small metastability.

Several recent modeling studies have been based on these results. The statistical-mathematical model presented by Ramanarayanan et al. (1984) and Zumstein and Rousseau (1987) can be used to recover growth kinetics from the resulting CSD in a batch crystallizer. The model, however, only allows the calculations for the case of a seeded crystallizer with no subsequent nucleation. Seeds were charged into the crystallizer (Berglund and Murphy, 1986) or contact nuclei were generated by dropping a rod on a well-faced parent crystal (Blem and Ramanarayanan, 1987).

It is the purpose of this work to develop a model based on the CCG formalism to relate the resulting CSD for both seeds and nuclei from a seeded batch crystallizer with nonnegligible nucleation to the seed size distribution, the initial size distribution of subsequently generated nuclei, and the growth rate distribution. This application is demonstrated for a batch sucrose crystallizer. In addition, the model allows recovery of the growth and nucleation rates from batch crystallizer CSD data. The application of the model to recover growth and nucleation rates is demonstrated for batch crystallization experiments with pure and glucose-containing aqueous fructose solutions. The results are compared with the unstirred solution studies from photomicroscopic experiments (Shiau and Berglund, 1987; Chu et al., 1989).

Model

A seeded batch crystallizer contains two types of crystals, seeds and subsequently generated nuclei, which can be represented by S crystals and N crystals, respectively (Jones and

Mullin, 1974). In the following development, one part represents the S crystals and the other part represents the subsequently generated N crystals. These two parts are subsequently summed to represent the overall CSD. The following assumptions are made in developing this model:

- Crystal breakage and agglomeration are negligible.
- The nuclei generated have an initial size distribution, which could be a function of supersaturation, but is independent of the growth rate distribution.
- The growth rate of a crystal is independent of its size.
- The CCG model is assumed applicable with negligible contributions from RF-type growth rate dispersion.

Therefore, the expression for the N crystals will be valid for an unseeded batch crystallizer, while the expression for the S crystals will apply to a seeded crystallizer without nucleation. The two will be combined for the general case.

N crystals

For a well-mixed, batch crystallizer, the number of nuclei generated at time t is given by

$$dN_N(t) = B^o(t)\,dt \tag{1}$$

Let $f_G(t;g)$ represent the distribution of growth rates for the crystals at t such that $f_G(t;g)dg$ is the fraction of the total number of crystals at t having a growth rate between g and $g + dg$. Further, let $f_{L_{N_o}}(t;\ell_{N_o})$ represent the distribution of initial sizes for the crystals generated at t such that $f_{L_{N_o}}(t;\ell_{N_o})d\ell_{N_o}$ is the fraction of the total number of nuclei generated at t having an initial size between ℓ_{N_o} and $\ell_{N_o} + d\ell_{N_o}$. Thus, the number of crystals, generated between t and $t + dt$ with a growth rate between g and $g + dg$ and an initial size between ℓ_{N_o} and $\ell_{N_o} + d\ell_{N_o}$, is given by

$$dN_N(t;\ell_{N_o}, g) = B^o(t)dt \cdot f_G(t;g)dg \cdot f_{L_{N_o}}(t;\ell_{N_o})d\ell_{N_o} \tag{2}$$

The size of crystals, generated at t with a growth rate g and an initial size ℓ_{N_o}, at T is given by

$$\ell_N(T;\ell_{N_o}, g) = \ell_{N_o}(t) + \int_t^T g(\theta)d\theta \tag{3}$$

where g is a function of θ and changes from t to T. Raising both sides to the jth power yields

$$\ell_N(T;\ell_{N_o}, g)^j = \left[\ell_{N_o}(t) + \int_t^T g(\theta)d\theta\right]^j \tag{4}$$

Expanding the righthand side of Eq. 4 in a binomial series yields

$$\ell_N(T;\ell_{N_o}, g)^j = \sum_{r=0}^{j}\binom{j}{r}\ell_{N_o}(t)^{j-r}\cdot\left[\int_t^T g(\theta)d\theta\right]^r \tag{5}$$

Therefore, the differential of the jth moment of the CSD, generated between t and $t + dt$ with a growth rate between g and $g + dg$ and an initial size between ℓ_{N_o} and $\ell_{N_o} + d\ell_{N_o}$, about the origin of the CSD at T can be written as

$$\begin{aligned}
&\ell_N(T;\ell_{N_o}, g)^j \cdot dN_N(t;\ell_{N_o}, g)\\
&\quad = B^o(t)\,dt \cdot f_G(\theta;g)\,dg \cdot f_{L_{N_o}}(t;\ell_{N_o})\,d\ell_{N_o} \cdot \ell_N(T;\ell_{N_o}, g)^j\\
&\quad = B^o(t)\,dt \cdot f_G(\theta;g)\,dg \cdot f_{L_{N_o}}(t;\ell_{N_o})\,d\ell_{N_o}\\
&\qquad \cdot \sum_{r=0}^{j}\binom{j}{r}\ell_{N_o}(t)^{j-r}\cdot\left[\int_t^T g(\theta)d\theta\right]^r\\
&\quad = B^o(t)\,dt \cdot \sum_{r=0}^{j}\binom{j}{r}\ell_{N_o}(t)^{j-r}\cdot f_{L_{N_o}}(t;\ell_{N_o})\,d\ell_{N_o}\\
&\qquad \cdot f_G(\theta;g)\,dg \cdot\left[\int_t^T g(\theta)d\theta\right]^r
\end{aligned} \tag{6}$$

where $f_G(t;g)$ has been replaced with $f_G(\theta;g)$ since $f_G(\theta;g)$ and g are functions of θ, which changes from t to T. Taking $f_G(\theta;g)\,dg$ inside the integral sign gives

$$f_G(\theta;g)\,dg \cdot\left[\int_t^T g(\theta)\,d\theta\right]^r = \left\{\int_t^T [g(\theta)^r \cdot f_G(\theta;g)\,dg]^{1/r}d\theta\right\}^r \tag{7}$$

Substituting Eq. 7 into Eq. 6 yields

$$\ell_N(T;\ell_{N_o}, g)^j \cdot dn_N(t;\ell_{N_o}, g) = B^o(t)\,dt \cdot \sum_{r=0}^{j}\binom{j}{r}\ell_{N_o}(t)^{j-r} \cdot f_{L_{N_o}}(t;\ell_{N_o})\,d\ell_{N_o} \cdot \left\{\int_t^T [g(\theta)^r \cdot f_G(\theta;g)\,dg]^{1/r}d\theta\right\}^r \tag{8}$$

Thus, the differential of the jth moment of the CSD, generated between t and $t + dt$ with all possible growth rates and all possible initial sizes, about the origin of the CSD at T can be written as

$$\ell_N(T)^j \cdot dn_N(t) = \int_{0}^{\infty}\int_{0}^{\infty} B^o(t)\,dt \cdot \sum_{r=0}^{j}\binom{j}{r}\ell_{N_o}(t)^{j-r} \cdot f_{L_{N_o}}(t;\ell_{N_o})\,d\ell_{N_o} \cdot \left\{\int_t^T [g(\theta)^r \cdot f_G(\theta;g)\,dg]^{1/r}d\theta\right\}^r \tag{9}$$

Noting that $\ell_{N_o}(t)$ and $g(\theta)$ are independent random variables (see assumption 2), Eq. 9 can be written as

$$\begin{aligned}
&\ell_N(T)^j \cdot dn_N(t) = B^o(t)\,dt\\
&\qquad \cdot \sum_{r=0}^{j}\binom{j}{r}\int_{0}^{\infty}\ell_{N_o}(t)^{j-r} \cdot f_{L_{N_o}}(t;\ell_{N_o})d\ell_{N_o}\\
&\qquad \cdot \left\{\int_t^T\left[\int_0^\infty g(\theta)^r \cdot f_G(\theta;g)\,dg\right]^{1/r}d\theta\right\}^r\\
&= B^o(t)\,dt \cdot \sum_{r=0}^{j}\binom{j}{r}M_{L_{N_o}}(t;j-r) \cdot\left[\int_t^T M_G(\theta;r)^{1/r}d\theta\right]^r
\end{aligned} \tag{10}$$

where

$$M_{L_{N_o}}(t;j-r) = \int_0^\infty \ell_{N_o}(t)^{j-r} \cdot f_{L_{N_o}}(t;\ell_{n_o})\, d\ell_N \qquad (11)$$

$$M_G(\theta;r) = \int_0^\infty g(\theta)^r \cdot f_G(\theta;g) dg \qquad (12)$$

Therefore, the jth moment of the nuclei CSD, generated from 0 to T, about the origin of the CSD at T is obtained by integrating from 0 to T thus,

$$M'_{L_N}(T;j) = \int_0^T \ell_N(T)^j \cdot dn_N(t)$$
$$= \int_0^T \left\{ B^o(t) \cdot \sum_{r=0}^{j} \binom{j}{r} M_{L_{N_o}}(t;j-r) \cdot \left[\int_t^T M_G(\theta;r)^{1/r}\, d\theta \right]^r \right\} dt \qquad (13)$$

since

$$M'_{L_{N_o}}(T;0) = \int_0^T B^o(t)\, dt \qquad (14)$$

The normalized jth moment of the CSD at T is

$$M_{L_N}(T;j) = \frac{1}{\int_0^T B^o(t)\, dt} \int_0^T \left\{ B^o(t) \cdot \sum_{r=0}^{j} \binom{j}{r} M_{L_{N_o}}(t;j-r) \cdot \left[\int_t^T M_G(\theta;r)^{1/r} d\theta \right]^r \right\} dt \qquad (15)$$

Equation 15 is the general result which is applicable to batch crystallization without seeding. Several special cases are given in Table 1.

S crystals

The number of seeds, charged into the crystallizer at $t = 0$ with a growth rate between g and $g + dg$ and an initial size ℓ_{s_o}, is given by

$$dN_s(0;\ell_{s_o}, g) = N_{s_o} \cdot f_G(0, g) dg \cdot f_{L_{s_o}}(0;\ell_{s_o}) \qquad (16)$$

where N_{s_o} is the total number of seeds charged into the crystallizer at $t = 0$, and $f_{L_{s_o}}(0;\ell_{s_o})$ represents the distribution of initial sizes for the seeds charged into the crystallizer at $t = 0$ such that $f_{L_{s_o}}(0;\ell_{s_o})d\ell_{s_o}$ is the fraction of the seeds having an initial size between ℓ_{s_o} and $\ell_{s_o} + d\ell_{s_o}$. $f_G(0;g)$ represents the distribution of growth rates for the seeds at $t = 0$ such that $f_G(0;g)dg$ is the fraction of the seeds having a growth rate between g and $g + dg$ at $t = 0$.

After considerable manipulation similar to that for Eq. 15 (shown in Appendix A), the normalized jth moment of the CSD at T is

$$M_{L_s}(T;j) = \sum_{r=0}^{j} \binom{j}{r} M_{L_{s_o}}(0;j-r) \cdot \left[\int_0^T M_G(\theta;r)^{1/r} d\theta \right]^r \qquad (17)$$

Equation 17 is valid for a seeded batch crystallizer without nucleation. A summary of special cases is given in Table 2.

N + S crystals

Combining Eqs. 15 and 17, the normalized jth moment of the entire CSD, including N crystals and S crystals, about the origin at T is

$$M_{L_{N+S}}(T;j) = \frac{1}{\int_0^T B^o(t) dt + N_{s_o}} \cdot \left[\int_0^T B(t) dt \cdot M_{L_N}(T;j) + N_{s_o} \cdot M_{L_S}(T;j) \right] \qquad (18)$$

Application of the Model

To model a batch crystallizer based on the model derived, it is necessary to solve the equation simultaneously with the mass

Table 1. Special Cases for Batch Crystallization without Seeding Resulting in Simplification of Eq. 15

Constant growth and nucleation rates	$M_{L_N}(T;j) = \sum_{r=0}^{j} \frac{1}{r+1} \cdot \binom{j}{r} M_{L_{N_o}}(T;j-r) \cdot M_G(T;r) \cdot T^r$
Monosized nuclei ($\ell_{N_o} = 0$)	$M_{L_N}(T;j) = \frac{1}{\int_0^T B^o(t)\, dt} \int_0^T \left\{ B^o(t) \cdot \sum_{r=0}^{j} \binom{j}{r} \ell_{N_o}^{j-r} \cdot \left[\int_t^T M_G(\theta;r)^{1/r}\, d\theta \right]^r \right\} dt$
Nuclei crystal born at zero size ($\ell_{N_o} = 0$)	$M_{L_N}(T;j) = \frac{1}{\int_0^T B^o(t)\, dt} \int_0^T \left\{ B^o(t) \cdot \left[\int_t^T M_G(\theta;r)^{1/r}\, d\theta \right]^r \right\} dt$
Constant growth and nucleation rates and monosized nuclei	$M_{L_N}(T;j) = \sum_{r=0}^{j} \frac{1}{r+1} \cdot \binom{j}{r} \ell_{N_o}^{j-r} \cdot M_G(T;r) \cdot T^r$
Constant growth and nucleation rates and nuclei born at zero size	$M_{L_N}(T;j) = \frac{M_G(T;j) \cdot T^j}{j+1}$

Table 2. Special Cases for Seeded Batch Crystallization without Nucleation Resulting in Simplification of Eq. 17

Constant growth rate	$M_{L_s}(T;j) = \sum_{r=0}^{j} \binom{j}{r} M_{L_{s_o}}(0;j-r) \cdot M_G(r) T^r$
Monosized seed ($\ell_s \neq 0$)	$M_{L_s}(T;j) = \sum_{r=0}^{j} \binom{j}{r} \ell_{s_o}^{j-r} \cdot [\int_0^T M_G(\theta;r)^{1/r} d\theta]^r$
Constant growth rate and monosized seeds	$M_{L_s}(T;j) = \sum_{r=0}^{j} \binom{j}{r} \ell_{s_o}^{j-r} \cdot M_G(r) \cdot T^r$

balance. The necessary equations can be summarized as follows:

Population balances (moment form)

For N crystals: Eq. 15
For S crystals: Eq. 17
For both N crystals and S crystals: Eq. 18

Mass balance

$$W_2(T) = W_2(O) + W_s - M_T(T) \cdot V(T) \tag{19}$$

Growth kinetics

Berglund and Murphy (1986) and Shiau and Berglund (1987) measured the mean growth kinetics of the variance of growth rate distribution for sucrose and fructose, respectively. In both cases, the mean growth rate can be correlated in an Arrhenius form, and the variance of growth rate distribution can be represented as a power law expression as follows:

$$\overline{G}(T) = Ae^{-Eg/R \cdot \mathrm{TEMP}} S(T)^m \tag{20}$$

$$\sigma_G^2(T) = a\,\overline{G}(T)^b \tag{21}$$

In terms of the moment form,

$$M_G(T;1) = \overline{G}(T) \tag{22}$$

and

$$\begin{aligned} M_G(T;2) &= \overline{G}(T)^2 + \sigma_G^2(T) \\ &= \overline{G}(T)^2 + a\overline{G}(T)^b \end{aligned} \tag{23}$$

In applying the model coupled with the mass balance equation, the third moment of growth rate distribution needs to be estimated from the knowledge of the first and second moments. The growth rate distribution can be fit to a gamma distribution (e.g., Larson et al., 1985) allowing the two parameters $\alpha(T)$ and $\beta(T)$ for the gamma distribution to be calculated from the mean and variance, thus

$$\beta(T) = \frac{\sigma_G^2(T)}{\overline{G}(T)} \tag{24}$$

$$\alpha(T) = \frac{\overline{G}(T)}{\beta(T)} \tag{25}$$

the third moment then may be written

$$M_G(T;3) = \alpha(T) \cdot (\alpha(T) + 1) \cdot (\alpha(T) + 2) \cdot \beta(T)^3 \tag{26}$$

Slurry density

$$M_T(T) = \rho \cdot k_v \cdot M_{L_{N+S}}(T;3) \cdot Num_{N+S}(T) \tag{27}$$

Nucleation kinetics

$$B^o(T) = k_N(T) \cdot M_T(T)^I \cdot S(T)^J \tag{28}$$

Free liquor volume

$$V(T) = \frac{V_T}{1 + k_v \cdot M_{L_{N+S}}(T;3) \cdot \mathrm{Num}_{N+S}(T)} \tag{29}$$

Number of N crystal and S crystals per unit free liquor volume

For N crystals:

$$\int_0^T B^o(t)dt$$

For S crystals:

$$\frac{N_{s_o}}{V(T)}$$

For both N crystals and S crystals:

$$\mathrm{Num}_{N+S}(T) = \int_0^T B^o(t)dt + \frac{N_{s_o}}{V(T)} \tag{30}$$

Example of Performance Analysis of a Batch Crystallizer

A crystallizer is initially seeded with crystals of uniform size. The conditions employed in this example are listed in Table 3. The crystallizer was simulated at a constant temperature of 40°C.

Figure 1 shows the desupersaturation curves, in which supersaturation in the case of GRD decreases faster than that of no GRD. Consequently, mean growth rate in the case of GRD decreases faster than that in the case of no GRD (Figure 2). The nucleation rate increases to a maximum and decreases for both

Table 3. Conditions Used in the Examples of a Batch Crystallizer for Sucrose

Parameters	Quantity
Sucrose crystal density, g/cm^3	1.588
Initial concentration, g sucrose/100 g soln	73
Sucrose solution, g	5,000
Seed size, μm	100
Seed loading, g	50
Birth size of nuclei, μm	0
Saturated sucrose conc., C^* in g sucrose/100 g soln and TEMP in K (Bates, 1942)	$c^* = 62.77 + 0.1760\,(\text{TEMP}-273.15) + 0.000344\,(\text{TEMP}-273.15)^2$
Mean growth rate kinetics in μm/min, TEMP in K, and C in g sucrose/100 g soln (Berglund, 1980)	$\overline{G} = 7.99 \times 10^{10} \exp\frac{-5.69 \times 10^7}{R \cdot \text{TEMP}} \cdot (C - C^*)^2$
Variance of growth rate distribution, $\overline{G}$ in μm/min and σ_G^2 in μm^2/min^2 (Berglund and Murphy, 1986)	$\sigma_G^2 = 0.286\,\overline{G}^{1.74}$
Nucleation rate, B^0 in #/cm^3 · min, $\overline{G}$ in μm/min, and g/cm^3 (Hartel, 1980)	$B^0 = 2.4 \times 10^{-8}\overline{G}^{1.5} M_T$

cases since mean growth rate decreases and suspension density increases in the crystallization process (Figure 3).

These results demonstrate that the model can be used to describe batch crystallization in the presence of nucleation. Furthermore, it can be used to establish the importance of growth rate dispersion in CSD establishment.

Recovery Growth and Nucleation Rates from Experimental Data

For the model presented to be applicable to a batch crystallizer, it is imperative that any nuclei generated obey the CCG model. The photomicroscopic studies by Shiau and Berglund (1987) and Chu et al. (1989) have confirmed that fructose crystals formed by contact nucleation follow the constant crystal growth model in pure fructose solution and in glucose containing fructose solution.

The approach to recovery of nucleation and growth rates will consider only the nuclei. This can easily be accomplished experimentally by using seeds which are much larger than the nuclei.

In the case of constant nucleation and growth rates, Eq. 15 reduces to (see Table 1).

$$M_L(j) = \sum_{r=0}^{j} \binom{j}{r} \cdot M_{L_o}(j-r) \cdot M_G(r) \cdot \frac{1}{r+1} \cdot T^r \qquad (31)$$

Here, $M_L(T;j)$, $M_{L_o}(t;j)$ and $M_G(\theta;j)$ are replaced with $M_L(j)$, $M_{L_o}(j)$ and $M_G(j)$, since these functions are no longer time-dependent.

A variety of birth size distributions of nuclei for constant nucleation and growth will be discussed in the following.

Case 1

Nuclei are born at zero size. Thus, Eq. 15 reduces to

$$M_L(j) = \frac{1}{j+1} \cdot M_G(j) \cdot T^j \qquad (32)$$

For $j = 1$ and $j = 2$

$$M_L(1) = \tfrac{1}{2} \cdot M_G(1) \cdot T \qquad (33)$$

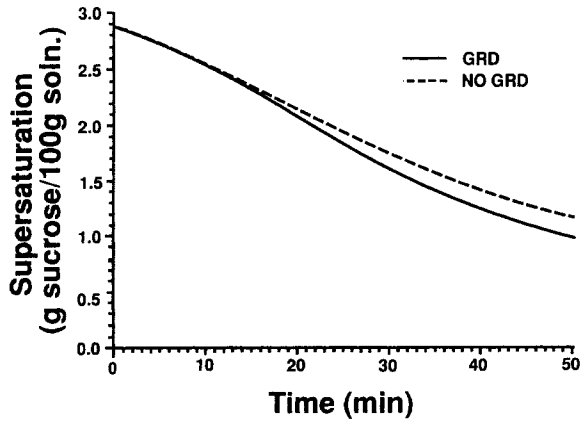

Figure 1. Supersaturation in an isothermal batch sucrose crystallizer ($T = 40$°C) as a function of time for simulations with and without effect of growth rate dispersion.

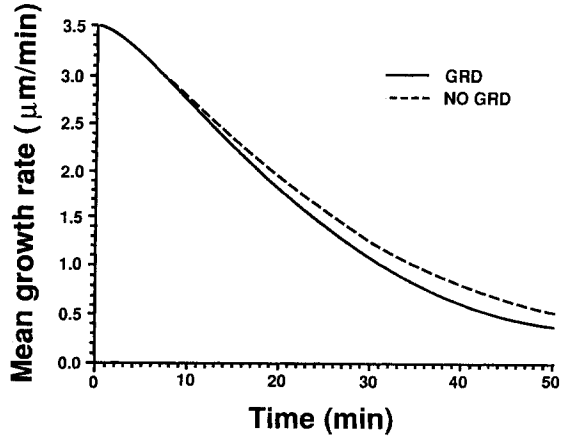

Figure 2. Mean crystal growth rate in an isothermal batch sucrose crystallizer ($T = 40$°C) as a function of time for simulations with and without effect of growth rate dispersion.

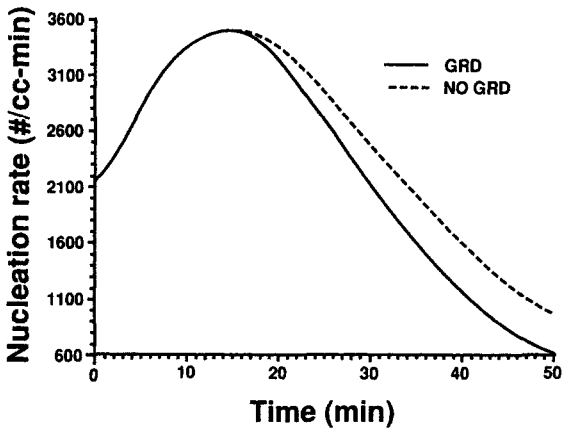

Figure 3. Nucleation rate in an isothermal batch sucrose crystallizer as a function of time for simulations with and without effect of growth rate dispersion.

and

$$M_L(2) = 1/3 \cdot M_G(2) \cdot T^2 \tag{34}$$

knowing that

$$M_G(1) = \overline{G} \tag{35}$$

and

$$M_G(2) = \overline{G}^2 + \sigma_G^2 \tag{36}$$

yields

$$M_L(1) = \overline{L} \tag{37}$$

and

$$M_L(2) = \overline{L}^2 + \sigma_L^2 \tag{38}$$

Equations 33 and 34 can be written as

$$\overline{L}^2 = 1/2 \cdot \overline{G} \cdot T \tag{39}$$

$$\overline{L}^2 + \sigma_L^2 = 1/3 \cdot T^2 \cdot (\overline{G}^2 + \sigma_G) \tag{40}$$

Therefore, a plot of $\overline{L}$ vs. $T/2$ passes through the origin with a slope of $\overline{G}$. Furthermore, a plot of $\overline{L}^2 + \sigma_L^2$ vs. $T^2/3$ passes through the origin with a slope of $\overline{G}^2 + \sigma_G^2$. Therefore, $\overline{G}$ and σ_G^2 can be determined from the CSD data.

For a batch crystallizer without agglomeration and particle breakage, the total number of crystals generated can be represented as

$$N = \int_0^T B^o(t)\, dt \tag{41}$$

at constant nucleation and growth conditions,

$$B^o = \frac{dN}{dT} \tag{42}$$

The nucleation rate can simply be evaluated from the rate of change of the total number of crystals.

Case 2

Nuclei are born at zero size and the smallest measurable size is L_{min}. Practically, any particle size analyzer has its smallest measurable size. Thus, nuclei have to grow up to some L_{min} to be measurable.

$$t_o = \frac{L_{min}}{G} \tag{43}$$

Here, $\overline{G}$ is the mean growth rate and t_o is the average time required for nuclei to grow into the smallest measurable size.

Starting with Eq. 15 and taking t_o into consideration, Eq. 15 can be modified for simplicity as

$$M'_L(j) \approx \frac{1}{\int_0^{T-t_o} B^o(t)dt} \cdot \int_0^{T-t_o} \left\{ B^o(t) \cdot \left[\int_t^T M_G(j)^{1/j} d\theta \right]^j \right\} dt = \frac{1}{j+1} \cdot M_G(j) \cdot \frac{T^{j+1} - t_o^{j+1}}{T - t_o} \tag{44}$$

where $M'_L(j)$ stands for the normalized jth moment of all the nuclei with sizes greater than L_{min} about the origin of CSD at T. For $j = 1$ and $j = 2$,

$$M'_L(1) = 1/2 \cdot M_G(1) \cdot (T + t_o) \tag{45}$$

and

$$M'_L(2) = 1/3 \cdot M_G(2) \cdot (T^2 + T \cdot t_o + t_o^2) \tag{46}$$

Substituting Eqs. 35 to 38 and 41, Eqs. 42 and 44 can be written as

$$\overline{L}' = \frac{L_{min}}{2} + \frac{\overline{G} \cdot T}{2} \tag{47}$$

$$\overline{L}'^2 + \sigma_{L'}^2 = \frac{(T^2 + T \cdot t_o + t_o^2)}{3} (\overline{G}^2 + \sigma_G^2) \tag{48}$$

where $\overline{L}'$ and $\sigma_{L'}^2$ are the mean size and the variance of nuclei distribution with sizes greater than L_{min} at T.

Therefore, a plot of $\overline{L}' - L_{min}/2$ vs. $T/2$ passes through the origin with a slope of $\overline{G}$. Once $\overline{G}$ is determined, t_o can be calculated from Eq. 43. Then, a plot of $\overline{L}'^2 + \sigma_{L'}^2$ vs. $(T^2 + T \cdot t_o + t_o^2)/3$ passes through the origin with a slope of $\overline{G}^2 + \sigma_G^2$. As in case 1, the growth parameters can be estimated from the CSD data.

The smallest particle capable of accurate detection by the size analysis technique is L_{min}, and thus total crystal counts give only N', the number of crystals with size greater than L_{min}.

$$N' \approx \int_0^{T - L_{min}/\overline{G}} B^o_{eff}(t)\, dt \tag{49}$$

In constant nucleation and growth condition,

$$N' \approx B^{o}_{\text{eff}} \cdot \left(T - \frac{L_{\min}}{\overline{G}}\right) \tag{50}$$

Therefore,

$$B^{o}_{\text{eff}} \approx \frac{dN'}{dT} \tag{51}$$

The nucleation rate can thus be approximately evaluated from the rate of change of the total number of crystals greater than $L_{\min}$. This gives an effective nucleation rate which is analogous to the one reported in linear extrapolation of data from continuous crystallizers (Hartel et al., 1980; Kuijvenhoven and deJong, 1982).

Case 3

Nuclei are born with an initial size distribution, and all are greater than $L_{\min}$. With this assumption, Eq. 1 reduces to

$$M_L(j) = \sum_{r=0}^{j} \binom{j}{r} \cdot M_{L_o}(j-r) \cdot M_G(r) \cdot \frac{1}{r+1} \cdot T^r \tag{52}$$

For $j = 1$ and $j = 2$

$$M_L(1) = M_{L_o}(1) + \tfrac{1}{2} \cdot M_G(1) \cdot T \tag{53}$$

and

$$M_L(2) = M_{L_o}(2) + M_{L_o}(1) M_G(1) \cdot T + \tfrac{1}{3} \cdot M_G(2) \cdot T^2 \tag{54}$$

Substituting Eqs. 35 to 38, and knowing

$$M_{L_o}(1) = \overline{L}_o \tag{55}$$

$$M_{L_o}(2) = \overline{L}_o^2 + \sigma_{L_o}^2 \tag{56}$$

Equations 55 and 56 can be written as

$$\overline{L} = \overline{L}_o + \tfrac{1}{2} \cdot \overline{G} \cdot T \tag{57}$$

$$\overline{L}^2 + \sigma_L^2 = \overline{L}_o^2 + \sigma_{L_o}^2 + \overline{L}_o \cdot \overline{G} \cdot T + \tfrac{1}{3} \cdot T^2 \cdot (\overline{G}^2 + \sigma_G^2) \tag{58}$$

Therefore, a plot of $\overline{L}$ vs. $T/2$ has a slope of $\overline{G}$ and an intercept of $\overline{L}_o$. A plot of $\overline{L}^2 + \sigma_L^2 - \overline{L}_o^2 - \overline{L}_o \cdot \overline{G} \cdot T$ vs. $T^2/3$ has a slope of $\overline{G}^2 + \sigma_G^2$ and an intercept of $\sigma_{L_o}^2$.

Since all nuclei are born with sizes greater than $L_{\min}$, the total particle counts give N, all the particles present. Therefore,

$$B^{o} = \frac{dN}{dT} \tag{59}$$

Case 4

Nuclei are born with an initial size distribution, and $\overline{L}_o$ is smaller than $L_{\min}$. (In the case that $\overline{L}_o$ is greater than $L_{\min}$, it will be treated as the same as case 3 for simplicity.) Therefore,

$$t_o = \frac{L_{\min} - \overline{L}_o}{\overline{G}} \tag{60}$$

where $\overline{G}$ is the mean growth rate, $\overline{L}_o$ is the mean birth size of nuclei, and t_o is the average time required for nuclei of size $\overline{L}_o$ to grow into the smallest measurable size.

Starting with Eq. 15 and taking t_o into consideration, the model equation can be approximately simplified as

$$M'_L(j) \approx \frac{1}{\int_0^{T-t_o} B^{o}(t)dt} \cdot \int_t^{T-t_o} \left\{ B^{o}(t) \cdot \sum_{r=0}^{j} \binom{j}{r} \cdot M_{L_o}(j-r) \cdot \left[\int_t^{T} M_G(r)^{1/r} d\theta \right]^r \right\} dt$$

$$= \sum_{r=0}^{j} \binom{j}{r} \cdot M_{L_o}(j-r) \cdot M_G(r) \cdot \frac{1}{r+1} \cdot \frac{T^{r+1} - t_o^{r+1}}{T - t_o} \tag{61}$$

where $M'_L(j)$ stands for the normalized jth moment of all the nuclei with sizes greater than $L_{\min}$ about the origin of CSD at T. For $j = 1$ and $j = 2$,

$$M'_L(1) = M_{L_o}(1) + \tfrac{1}{2} \cdot M_G(1) \cdot (T + t_o) \tag{62}$$

and

$$M'_L(2) = M_{L_o}(2) + M_{L_o}(1) \cdot M_G(1) \cdot (T + t_o) + \tfrac{1}{3} \cdot M_G(2) \cdot (T^2 + T + t_o + t_o^2) \tag{63}$$

Substituting Eqs. 35 to 38, 50, 51 and 54, Eqs. 57 and 58 can be written as

$$\overline{L}' = \frac{L_{\min} + \overline{L}_o}{2} + \frac{\overline{G} \cdot T}{2} \tag{64}$$

$$\overline{L}'^2 + \sigma_{L'}^2 = \overline{L}_o^2 + \sigma_{L_o}^2 + \overline{L}_o \cdot \overline{G} \cdot (T + t_o) + \frac{(T^2 + T \cdot t_o + t_o^2)}{3} \cdot (\overline{G}^2 + \sigma_G^2) \tag{65}$$

Therefore, a plot of $\overline{L}' - L_{\min}/2$ vs. $T/2$ has a slope of $\overline{G}$ and an intercept of $L_o/2$. Once $\overline{G}$ is determined, t_o can be calculated from Eq. 60. Then, a plot of $\overline{L}'^2 + \sigma_{L'}^2 - \overline{L}_o^2 - \overline{L}_o \cdot \overline{G} \cdot (T + t_o)$ vs. $(T^2 + T \cdot t_o + t_o^2)/3$ has a slope of $\overline{G}^2 + \sigma_G^2$ and an intercept of $\sigma_{L_o}^2$.

In this case, the total crystal counts give only N', the number of crystals with size greater than $L_{\min}$.

$$N' \approx \int_0^{T-(L_{\min}-\overline{L}_o/\overline{G})} B^{o}_{\text{eff}}(t)dt \tag{66}$$

In the case of constant growth and nucleation,

$$N' \approx B^{o}_{\text{eff}} \cdot \left(T - \frac{L_{\min} - \overline{L}_o}{\overline{G}}\right) \tag{67}$$

Therefore,

$$B^{o}_{\text{eff}} \approx \frac{dN'}{dT} \tag{68}$$

The effective nucleation rate can thus be evaluated from the rate of change of the total number of crystals greater than $L_{\min}$.

Experimental Procedure

A series of batch experiments were performed in a 1.0 L, agitated, baffled vessel. The crystallizer was immersed in a constant-temperature bath and all runs were carried out isothermally. Initial supersaturation was achieved by slow cooling of a solution saturated at an elevated temperature. When the working temperature was attained, 10 g of presized (200–500 μm) and cured seeds were charged into the crystallizer. Seed size was chosen such that growing seed crystals would be at least an order of magnitude larger than nuclei. The current study concentrated on the analysis of the nuclei generated only. The seeds were cured by keeping them in a small amount (about 50 mL) of solution saturated at the working temperature prior to the experiments to prevent secondary nucleation by initial breeding. The beaker containing the seeds and solution was preheated 5°C above the saturation temperature of the solution for about 20 minutes. The seeds dissolved slightly since the solution was undersaturated at this condition. The solution containing seeds was cooled to the working temperature and charged into the crystallizer at the start of the run. The impeller speed was kept at 480 rpm, which was observed adequate to keep the seeds uniformly dispersed in the solution. Small volume samples of the solution were removed from the crystallizer to determine the particle counts and the CSD of the nuclei through image analysis at regular intervals during the course of the run. Sample measurements were taken within 10–20 hours depending on the supersaturation and impurity ratio so as not to change the supersaturation drastically. The experimental conditions are given in Table 4.

Data Analysis

Photomicrographs were taken of the samples from the crystallizer. The volume of the solution taken in a picture was estimated by the area of the picture multiplied by the thickness of the solution chamber (about 500 μm). Therefore, the number of nuclei per unit volume and the mean and variance of the CSD of the nuclei were determined. The raw data obtained from each experiment consisted of a series of photographs at various times. The negatives of the photographs were projected to enlarge them for measurement. An image analyzer was used to determine the area of each crystal in the enlargement. The characteristic size was taken as the equivalent circular diameter, which could be transformed to the geometric mean size by multiplying $\sqrt{\pi}/2$.

The smallest measurable size for the image analyzer under 100 × magnification was taken as 5 μm. Nuclei were considered born at near zero size; therefore, the analysis in case 2 was applied to determine the growth kinetics and nucleation rate for each experimental condition.

Table 4. Range of Experimental Variables for Batch Fructose Experiments

Operating temp., °C	40
Stirrer speed, rpm	480
Relative supersaturation	0.003 ~ 0.042
Impurity ratio, glucose/water, g/g	0 ~ 0.9
Seeding, charge, g	10
Seed, size, μm	200–500
Run time, h	10–20

Results and Discussion

Growth kinetics

Figure 4 shows an example of $\overline{L}' - L_{\min}/2$ plotted vs. $T/2$ with the slope equal to $\overline{G}$, and Figure 5 shows an example of $\overline{L'^2} - \sigma^2_{L'}$ plotted vs. $(T^2 + T \cdot t_o + t_o^2)/3$ with the slope equal to $\overline{G}^2 + \sigma^2_G$ for pure fructose solution at 3°C supercooling at 40°C. Linear relations can be approximated from these two figures as predicted from the analysis in case 2.

The effects of glucose on growth kinetics of fructose crystals were also examined. Glucose was added to pure fructose solution at various impurity/water ratios (I/W). Plots similar to Figures 4 and 5 were made for the fructose solutions at various levels of impurity and degrees of supercooling at 40°C. $\overline{G}$ and σ^2_G were determined at each experimental conditions from those plots.

Figure 6 shows the comparison of the mean growth rates obtained from the batch crystallization experiments for different levels of impurity at 40°C with the results determined from the photomicroscopic studies for pure fructose solutions (Shiau and Berglund, 1987) and glucose-containing fructose solutions (Chu et al., 1989). As seen in the figure, they are in good agreement. This agreement between such different experiments is probably due to the high viscosity of the fructose solutions such that the stirring provided by the impeller in the batch crystallizer does not affect its volume diffusion limitation during the process of crystallization. (In fact, those small nuclei might essentially flow around the crystallizer with the solution: i.e., the relative motion between nuclei and solution may be negligible.)

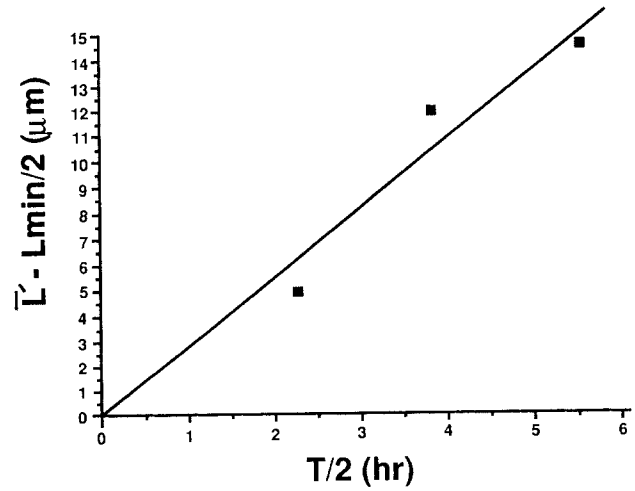

Figure 4. Typical plot of $\overline{L}' - L\,\text{min}/2$ vs. $T/2$ for contact nuclei formed during seeded batch fructose crystallization.

The experiment was conducted with pure solution at 40°C and 3°C undercooling. $L_{\min}$ was 5 μm

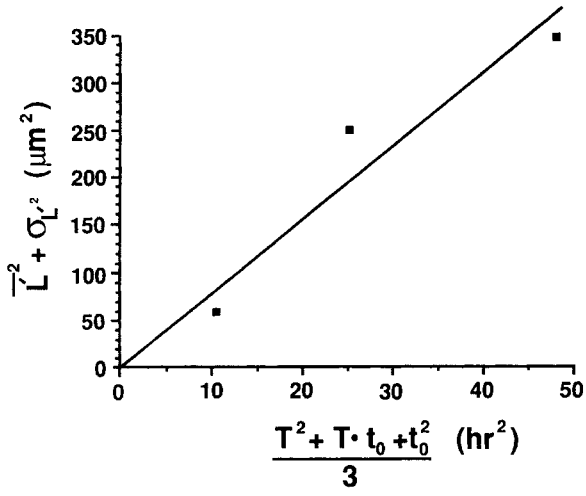

Figure 5. Typical plot of $\overline{L}'^2 + \sigma_{L'}^2$ vs. $(T^2 + T \cdot t_o + t_o^2)/3$ for contact nuclei formed during seeded batch fructose crystallization.

The experiment was conducted with pure solution at 40°C and 3°C undercooling. Other parameters include: $L_{min} = 5$ μm; $t_o = L_{min}/\overline{G} = 1.81$ h; $\overline{G} = 2.76$ μm/h (from results of Figure 4)

The solubility data were taken from circular C440 of the National Bureau of Standards (Bates, 1943). Since the effects of glucose on fructose solubility are not clear, the same definition for relative supersaturation is used in the fructose solution with glucose, i.e., as if the presence of glucose does not affect solubility of fructose in water. It was observed, however, that nuclei could be generated and start to grow only when S reached a critical value at each condition and that critical value of S increased as I/W was increased. This phenomenon indicates an increase of solubility at increase of I/W, which is consistent with the results from the photomicroscopic studies (Chu et al., 1989).

The variances of growth rates were plotted against mean growth rates for each experimental condition for comparison with the results obtained from the photomicroscopic studies from pure fructose solutions (Shiau and Berglund, 1987) and glucose-containing fructose solutions (Chu et al., 1989) in Figure 7. The data from the batch experiments were comparable, but quite widely scattered compared to the results from the photomicroscopic studies. The scatter is probably due to the limited nuclei data used for analysis in these batch experiments. The variances of growth rate distributions in the photomicroscopic studies were determined from the growth rate distributions of the nuclei generated by contact nucleation through sliding a parent crystal against a glass plate. The variances in the batch experiments, however, were predicted from the change of the means and variances of the nuclei generated constantly by contact nucleation through the stirring of the impeller in the solutions; therefore, a sufficient amount of nuclei data is critical to represent the true mean and variance of the sizes of the nuclei generated constantly in the solutions.

Unlike photomicroscopic experiments, in which the contacting is accomplished by sliding a parent crystal against cover glass without measuring the energy of contacting, the contacting of crystals is caused by the impeller in the seeded solutions during the batch crystallization experiments. Since the energy of contact can be estimated from the stirring rate of the impeller in batch crystallization experiments, this could allow the effects of contact energy on mean growth rates and variances of growth rate distributions to be studied.

Nucleation

Figure 8 shows the relationship between effective nucleation rate and mean growth rate for anhydrous fructose at 40°C. The effective nucleation rate was determined by Eq. 51. Since the major effect of glucose on fructose crystal growth is the increase of solubility as seen in the present batch studies and the photomicroscopic studies (Chu et al., 1989), it would be reasonable to predict the similar phenomenon on the nucleation. The effective nucleation rate was correlated by an empirical power law expression with the mean growth rate.

$$B^o = 5.0 \times 10^2 \, \overline{G}^{1.5} \tag{69}$$

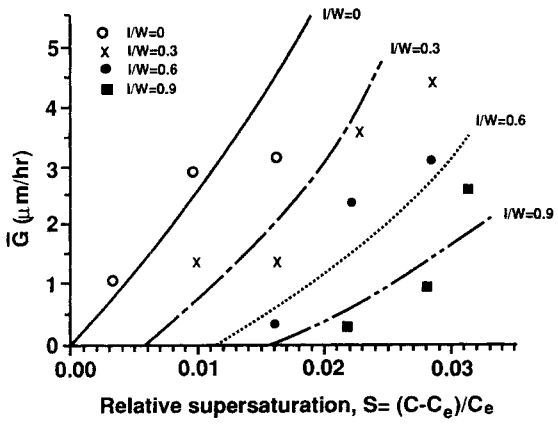

Figure 6. Comparison of the mean growth rates determined for fructose nuclei in the current batch crystallization experiments with those obtained in previous photomicroscopic studies.

($I/W = 0$, Shiau and Berglund, 1987; $I/W = 0.3$, 0.6, and 0.9, Chu et al., 1989)

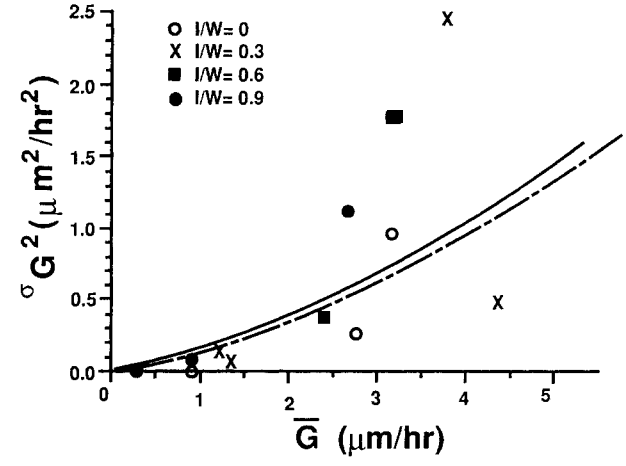

Figure 7. Variances of the nuclei growth rate distribution determined for fructose nuclei: in the current batch crystallization experiments vs. in previous photomicroscopic studies.

($I/W = 0$, Shiau and Berglund, 1987; $I/W = 0.3$, 0.6, and 0.9, Chu et al., 1989)

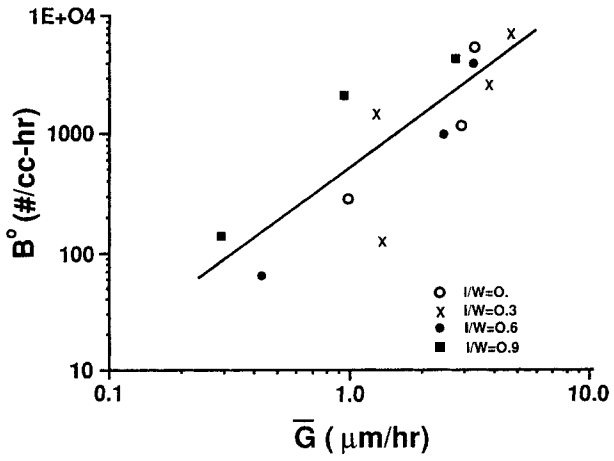

Figure 8. Nucleation rate vs. mean growth rate for fructose contact nuclei in seeded batch nucleation experiments at 40°C.

Summary

A method has been presented for both modeling and recovery of kinetic data from batch crystallizers. The results illustrate that the technique can potentially be used for treating real experimental data.

Acknowledgment

This work was supported by the National Science Foundation through grant number CPE-8412101.

Notation

a,b = constants in Eq. 21
$B^o(t)$ = nucleation rate at time t, nuclei/cm^3 · h
$B^o_{\text{eff}}(t)$ = nucleation rate at t, nuclei/cm^3 · h
C = solute concentration, g solute/100 g solution
C^* = saturated solute concentration, g solute/100 g solution
$C^*(t)$ = saturated solute concentration at t, g solute/100 g solution
E_G = activation energy, cal/gmol
$f_G(t;g)$ = probability density function for growth rate at t
$f_{L_{N_o}}(t;\ell_{N_o})$ = probability density function for initial sizes of crystals generated at time t
$f_{L_{s_o}}(0;\ell_{s_o})$ = probability density function for initial size of S crystals at $t = 0$
$\overline{G}$ = mean linear growth rate, μm/h
$\overline{G}(T)$ = mean linear growth rate at T, μm/h
g = linear crystal growth rate, μm/h
$g(t)$ = individual linear growth rate at t, μm/h
I = nucleation rate order with respect to M_T
J = nucleation rate order with respect to S
k_N = nucleation rate parameter
k_V = volume shape factor
L_{min} = smallest measurable size, μm
$\overline{L}$ = mean of the crystal size distribution, μm
$\overline{L}'$ = mean of the crystal size distribution with size greater than L_{min}, μm
$\overline{L}_o$ = mean of the birth size distribution, μm
ℓ_N = crystal size of N crystals, μm
ℓ_{N_o} = initial size of N crystals initially charged into crystallizer at $t = 0$ μm
$\ell_{N_o}(t)$ = birth size of N crystals generated at t, μm
$\ell_N(t)$ = size of N crystals at time t_j, μm
$\ell_N(t;\ell_{N_o}, g)$ = size of N crystals at time t with initial size ℓ_{N_o} and growth rate g
$\ell_{s_o}(t)$ = initial size of S crystals initially charged into crystallizer at time t, μm
$M_G(t;j)$ = normalized jth moment of growth rate distribution about the origin at t
$M_G(j)$ = normalized jth moment of growth rate distribution about the origin
$M'_L(j)$ = normalized jth moment of all the crystals greater than L_{min}, generated from 0 to T, about the origin
$M_{L_N}(T;j)$ = normalized form of $M_{L'_N}(T;j)$
$M'_{L_N}(T;j)$ = jth moment of the nuclei size distribution generated from to T, about the origin of the CSD at T, μm^j
$M_{L_o}(j)$ = normalized jth moment of the birth size distribution about Rrigin
$M_{L_{N_o}}(t;j)$ = jth moment of the nuclei size distribution about the origin at time t, μm^j
$M_{L_s}(T;j)$ = normalized jth moment of all the S crystals, charged into crystallizer at $t = 0$, about the origin at T
$M'_{L_s}(T;j)$ = jth moment of all the S crystals, charged into crystallizer at $t = 0$, about the origin of T, μm^j
$M_{L_{s_o}}(0;j)$ = normalized jth moment of all the S crystals, charged into crystallizer at $t = 0$, about the origin at $t = 0$.
$M_{L_{N+S}}(T;j)$ = normalized jth moment of all the $N + S$ crystals in the crystallizer about the origin at T
M_T = suspension density for N and S crystals at t, g/cm^3
n_N = population density of crystals, #/μm · cm^3
$N_N(t)$ = number density of N crystals at t, #/μm · cm^3
$N_S(t)$ = number density of S crystals at t, #/μm · cm^3
N_{s_o} = number of crystals charged into the crystallizer at $t = 0$, #/cm^3
$\text{Num}_{N+S}(t)$ = number of $N + S$ crystals per unit volume at t
R = ideal gas constant, 8,314 m^3 · Pa / kmol · K
$S(T)$ = supersaturation $[= c(t) - c^*(t)]$ g solute/100 g solution
T = time at which the CSD is observed or measured, h
t = time designating which quantities are a function of time, h
t_o = average time required for nuclei to grow into the smallest measurable size
TEMP = temperature, K
$V(T)$ = free liquor volume, cm^3
V_T = crystallizer volume, cm^3
W_s = seed loading, g
$W_2(0)$ = initial solute in the crystallizer, g
$W_2(T)$ = solute in the crystallizer at t, g

Greek letters

$\alpha(t), \beta(t)$ = parameters in gamma distribution at t
ρ = crystal density, g/cm^3
σ_G^2 = variance of growth rate distribution, μm^2/h^2
$\sigma_G^2(T)$ = variance growth rate distribution at t, μm^2/h^2
σ_L^2 = variance of crystal size distribution, μm^2
$\sigma_{L'}^2$ = variance of crystal size distribution with sizes greater than L_{min}, μm^2
$\sigma_{L_o}^2$ = variance of birth size distribution, μm^2
τ = mean retention time, h

Literature Cited

Bates, F. J., *Polarimetry, Saccharimetry and the Sugars*, U.S. Government Printing Off., Washington, DC (1942).

Berglund, K. A., "Summary of Recent Research on Growth Rate Dispersion of Contact Nuclei," *Chem. Eng. Commun.*, **41**, 357 (1986).

Berglund, K. A., E. L. Kaufman, and M. A. Larson, "Growth of Contact Nuclei on Potassium Nitrate," *AIChE J.*, **29**, 867, (1983).

Berglund, K. A., and M. A. Larson, "Growth and Growth Dispersion of Contact Nuclei," World Cong. Chem. Eng., Montreal (1981).

Berglund, K. A., and V. G. Murphy, "Modeling Growth Rate Dispersion in a Batch Sucrose Crystallizer," *Ind. Eng. Chem. Fundam.*, **25**, 174 (1986).

Blem, K. E., and K. A. Ramanarayanan, "Generation and Growth of Secondary Ammonium Dihydrogen Phosphate Nuclei," *AIChE J.*, **33**, 677 (1987).

Chu, Y. D., L. D. Shiau, and K. A. Berglund, "Effects of Impurities on Crystal Growth in Fructose Crystallization," *J. Cryst. Growth*, **97**, 689 (1989).

Garside, J., "Industrial Crystallization from Solution," *Chem. Eng. Sci.*, **40**, 3 (1985).
Garside, J., and M. A. Larson, "Direct Observation of Secondary Nuclei Production," *J. Cryst. Growth*, **43**, 694 (1978).
Hartel, R. W., "A Kinetic Study of the Nucleation and Growth of Sucrose Crystals in a Continuous Cooling Crystallizer," PhD Diss., Colorado State U., Fort Collins, CO (1980).
Jones, A. G., and J. W. Mullin, "Programmed Cooling Crystallization of Potassium Sulphate Solutions," *Chem. Eng. Sci.*, **29**, 105 (1974).
Kuijvenhoven, L. J., and E. J. deJong, "The Kinetics of Continuous Sucrose Crystallization" *Industrial Crystallization*, S. J. Jancic and E. J. deJong, eds., North Holland Publishing, 253 (1982).
Larson, M. A., E. T. White, K. A. Ramanarayanan, and K. A. Berglund, "Growth Rate Dispersion in MSMPR Crystallizers," *AIChE J.*, **31**, 90 (1985).
Ramanarayanan, K. A., "Production and Growth of Contact Nuclei," PhD Diss., Iowa State U., Ames, IA (1982).
Ramanarayanan, K. A., K. Athrea, and M. A. Larson, "Statistical-Mathematical Modeling of CSD in Continuous and Batch Crystallizers," *AIChE Symp. Ser.*, **80**, 76 (1984).
Randolph, A. D., and E. T. White, "Modeling Size Dispersion in the Predication of Crystal-Size Distribution," *Chem. Eng. Sci.*, **32**, 1067, (1977).
Shiau, L. D., and K. A. Berglund, "Growth Kinetics of Fructose Crystals Formed by Contact Nucleation," *AIChE J.*, **33**, 1028 (1987).
Zumstein, R. C., and R. W. Rousseau, "Growth Rate Dispersion by Initial Growth Rate Distributions and Growth Rate Fluctuations," *AIChE J.*, **33**, 121 (1987).

Appendix: Development of Eq. 17

Starting with Eq. 16, $dN_s(0;\ell_{s_o},g) = N_{s_o} \cdot f_G(0,g)dg \cdot f_{L_{s_o}}(0;\ell_{s_o})$, the size of seeds, charged into the crystallizer at $t = 0$ with a growth rate g and an initial size ℓ_{s_o} at T is given by:

$$\ell_s(T;\ell_{s_o},g) = \ell_{s_o}(0) + \int_0^T g(\theta)d\theta \tag{A1}$$

So,

$$\ell_s(T;\ell_{s_o},g)^j = \left[\ell_{s_o}(0) + \int_0^T g(\theta)d\theta\right]^j \tag{A2}$$

Expanding the righthand side of Eq. A2 in a binomial series yields

$$\ell_s(T;\ell_{s_o},g)^j = \sum_{r=0}^{j}\binom{j}{r}\ell_{s_o}(0)^{j-r}\cdot\left[\int_0^T g(\theta)d\theta\right]^r \tag{A3}$$

Therefore, the jth moment of seeds, with a growth rate g and initial size ℓ_{s_o}, about the origin of CSD at T is

$$\begin{aligned}\ell_s(T;\ell_{s_o},g)^j \cdot dn_s(\ell_o,g) &= N_{s_o}\cdot f_G(\theta;g)dg\cdot f_{L_{s_o}}(0,\ell_{s_o})d\ell_{s_o}\cdot\ell_s(T;\ell_{s_o},g)^j\\ &= N_{s_o}\cdot f_G(\theta,g)dg\cdot f_{L_{s_o}}(0;\ell_{s_o})d\ell_s\cdot\sum_{r=0}^{j}\binom{j}{r}\ell_{s_o}(0)^{j-r}\\ &\quad\cdot\left[\int_0^T g(\theta)d\theta\right]^r = N_{s_o}\cdot\sum_{r=0}^{j}\binom{j}{r}\ell_{s_o}(0)^{j-r}\\ &\quad\cdot f_{L_{s_o}}(0;\ell_{s_o})d\ell_s\cdot f_G(\theta;g)dg\cdot\left[\int_0^T g(\theta)d\theta\right]^r\end{aligned} \tag{A4}$$

Here, $f_g(0;g)$ has been replaced with $f_G(\theta;g)$, since $f_G(\theta;g)$ and g are functions of θ, which changes from 0 to T. Taking $f_G(\theta;g)dg$ inside the integral sign yields

$$f_G(\theta;g)dg\cdot\left[\int_0^T g(\theta)d\theta\right]^r = \left\{\int_0^T [g(\theta)^r\cdot f_G(\theta;g)dg]^{1/r}d\theta\right\}^r \tag{A5}$$

Substituting Eq. A5 into Eq. A4 yields

$$\ell_s(T;\ell_{s_o},g)^j\cdot dn_s(\ell_o,g) = N_{s_o}\cdot\sum_{r=0}^{j}\binom{j}{r}\ell_{s_o}(0)^{j-r}\cdot f_{L_{s_o}}(0;\ell_{s_o})\cdot[(g(\theta)^r\cdot f_G(\theta;g)dg)^{1/r}d\theta]^r \tag{A6}$$

Thus, the jth moment of all the seeds (with all possible growth rates and all possible initial sizes) about the origin of CSD at T is

$$M'_{L_s}(T;j) = \int_{(\ell_{s_o})}^{\infty}\int_{(g)}^{\infty} N_{s_o}\cdot\sum_{r=0}^{j}\binom{j}{r}\ell_{s_o}(0)^{j-r}\cdot f_{L_{s_o}}(0;\ell_{s_o})d\ell_{s_o}\cdot\left\{\int_{(\theta)}^{T}[g(\theta)^r\cdot f_G(\theta;g)dg]^{1/r}d\theta\right\}^r \tag{A7}$$

Noting that $\ell_{s_o}(0)$ and $g(\theta)$ are independent random variables, Eq. A7 can be rewritten as

$$\begin{aligned}M'_{L_s}(T;j) &= N_{s_o}\cdot\sum_{r=0}^{j}\binom{j}{r}\int_{(\ell_{s_o})}^{\infty}\ell_{s_o}(0)^{j-r}\cdot f_{L_{s_o}}(0;\ell_{s_o})d\ell_{s_o}\\ &\quad\cdot\left\{\int_{(\theta)}^{T}\left[\int_{(g)}^{\infty} g(\theta)^r\cdot f_G(\theta;g)dg\right]^{1/r}d\theta\right\}^r\\ &= N_{s_o}\cdot\sum_{r=0}^{j}\binom{j}{r}M_{L_{s_o}}(0;j-r)\\ &\quad\cdot\left[\int_0^T M_G(\theta;r)^{1/r}d\theta\right]^r\end{aligned} \tag{A8}$$

where

$$M_{L_{s_o}}(0;j-r) = \int_0^{\infty}\ell_{s_o}(0)^{j-r}\cdot f_{L_{s_o}}(0;\ell_{s_o})d\ell_{s_o} \tag{A9}$$

Since N_{s_o} is the total number of seeds, the normalized jth moment of the CSD at T is

$$M_{L_s}(T;j) = \sum_{r=0}^{j}\binom{j}{r}M_{L_{s_o}}(0;j-r)\cdot\left[\int_0^T M_G(\theta;r)^{1/r}d\theta\right]^r \tag{A10}$$

Equation A10 is the same as Eq. 17.

Manuscript received Nov. 21, 1989, and revision received Aug. 9, 1990.